Micron 126 (2019) 102748

Contents lists available at ScienceDirect

Micron

journal homepage: www.elsevier.com/locate/micron

Structure, morphology and composition of fur on different parts of reindeer (*Rangifer Tarandus*) foot

Rui Zhang[a,*], Guoyu Li[a], Ruiduo Pan[b], Qiang Wang[b], Jianqiao Li[a]

[a] Key Laboratory of Bionic Engineering, Ministry of Education, Jilin University, Changchun, China
[b] Department of Radiology, the First Hospital, Jilin University, Changchun, China

ARTICLE INFO

Keywords:
Furs of reindeer foot
Structure and morphology
Composition
Functional analysis
Experimental measurement

ABSTRACT

In the long-distance migration of reindeer in winter, furs of reindeer foot, as the part in direct contacting with the external environment, can play the role of protection and heat preservation. With furs on different parts of the right posterior foot (fibular side, tibial side and planta pedis) as research objects, the microstructure of reindeer foot furs was observed with a scanning electron microscope. The image displayed that the reindeer foot furs was divided into 3 layers, namely cuticular layer, cortical layer and medulla layer. It was observed from the fur surface that the scales of fur on tibial side had smooth edge, with the scale structure in mosaic and coronary types. The scale structure of furs on the other parts showed the irregular waves due to abrasion to different degrees. From the cross-section view of fur, there was a non-medullated segment on the medial part of fur on planta pedis. The medulla layer of fibular and tibial sides showed a porous foam structure. The medulla index (MI) of fur on fibular side and tibial side at distal part was 70.35% and 81.79%, respectively, and MI at medial part was 77.88% and 88.08%. The composition of reindeer foot fur was measured through infrared spectroscopy and energy spectrum analysis respectively. The element contents of foot fur varied on different parts. The content of sulfur of the furs on planta pedis was higher than that on other parts. The research results can provide foundations for the functional study and bionic design of reindeer foot furs during long distance migration and swimming.

1. Introduction

For all animals, the fur, as cuticular derivative, is unique to mammals (Noback, 2010), which has attracted widespread attention of researches in fields of morphology, auxanology (Meyer et al., 2010) and forensic medicine, etc. The structure of fur, with diversity, is usually the columnar structure that is easy to deform. In morphology, the fur can be divided into 3 layers, i.e. cuticular layer, cortical layer and medulla layer (nonexistent for some animals).

The macro and micro characteristics have been widely applied to fur identification and functional study of environmental adaptation. Researchers used to observe the surface structure of animal fur with an optical microscope (Wallis, 1993; Oli, 1993; Taru and Backwell, 2013), but now, the observation with greater magnification times and higher resolution ratio can be achieved through new technologies provided by scanning electron microscope (SEM) (Erdoğan et al., 2016; Aris and George, 2008; Alam et al., 2019). The micro technology is often used to observe the form of fur, such as diameter of fur, diameter and structure of medulla layer, and type of cuticular layer, etc. Hausman, based on the study on micro characteristics of beast fur, firstly proposed and then compared the interspecific difference of fur in microstructure, which showed the significance of classification (Hausman, 1920). Andereson analyzed the frequency and complexity of scales on fur surface and other relevant indexes through computer technology and also classified and identified 13 galagos of Galago (Anderson, 2001).

The researches on animal fur primarily focused on its structural characteristics, classification and identification, etc (Ahmed et al., 2018). Meanwhile, some scholars combined the researches on morphological structure and functional relationship of fur, mainly including heat insulation, protection, waterproofness, flight and other aspects of animal fur (Scholander et al., 1950; Rymer et al., 2007; Anzures et al., 2019). Meyer et al. (Meyer et al., 2006) compared the fur scales of mammals on the basis of morphology and pointed out the uniformity in structure and function of fur scales. Cain thought that the fur color is a vital determinant for animals to obtain solar energy (Cain et al., 2006) and the fur has different thermal insulation properties on different body parts (Jacobsen, 1980). For animals with close genetic relationship and the same individual on different developmental stages, the fur structure

* Corresponding author at: Key Laboratory of Bionic Engineering, Ministry of Education, Jilin University, No. 5988 Renmin Street, Changchun, 130022, China.
E-mail address: zhangrui@jlu.edu.cn (R. Zhang).

https://doi.org/10.1016/j.micron.2019.102748
Received 7 August 2019; Received in revised form 31 August 2019; Accepted 1 September 2019
Available online 05 September 2019
0968-4328/

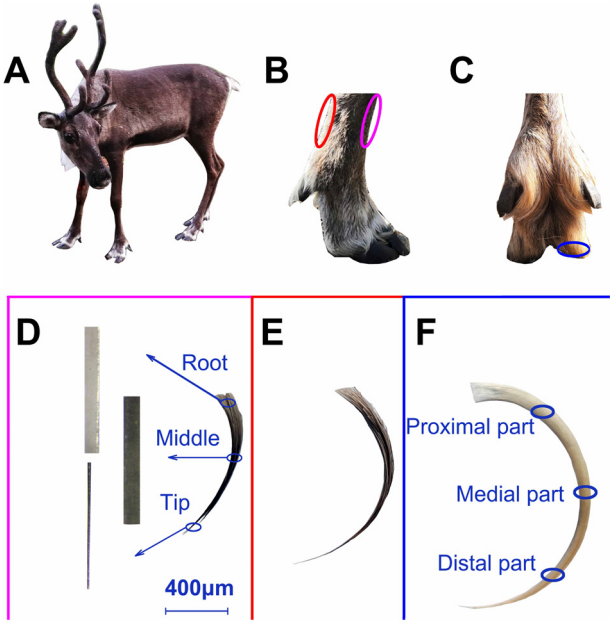

Fig. 1. Foot of reindeer and fur in fibular side, tibial side and planta pedis. A. Reindeer. B. Side view of foot. The pink circle refers to the fur of fibular side and the red one refers to the fur of tibial side. C. Upward view of foot. The blue circle refers to the fur of planta pedis. D. Fur of fibular side. E. Fur of tibial side. F. Fur of planta pedis. (For interpretation of the references to colour in this figure legend, the reader is referred to the web version of this article).

may have significant difference. Hence, the fur can adapt to the environment very well. At present, the morphological structure of fur has been studied systematically, but not functionally. Polar animals have formed a body structure that can adapt to the environment well in the process of natural evolution (Gilg et al., 2012), so it is necessary to study the fur of polar animals functionally

Reindeer belong to the migratory animal in polar environment (Payne et al., 2005), with their foot structure suitable for the migration on thick and soft snowfield (Currey, 1999; Nakayama et al., 2004). The hoof bolster of reindeer will contract and fasten in winter. Besides, the contraction of hoof bolster and exposure of hoof edge are conducive to their walking on the ice to prevent slippage (Banfieldal, 1957). Reindeer migrate not only in winter on snow-covered soil or ice, but also in spring and autumn in the steppe tundra and in wooded areas (Wareing et al., 2011). They also swim long distances (Ricca et al., 2012). When reindeer walk on the ice and snow, the bristle of high density will form a layer of close-knit “furbrush” around hoof bolster. Moreover, the foot fur will contact the ground directly to increase the contact area with ground and reduce the kinetic pressure of hooves. These features can enhance the long-distance migration capability of reindeer. Furthermore, there is no functional study on the foot fur of reindeer. In terms of structure, the animal species can be identified according to the morphological features of fur, which makes the morphological test of fur become an important method in the field of forensic medicine (Sato et al., 2006).Is there any special structure on the reindeer fur?

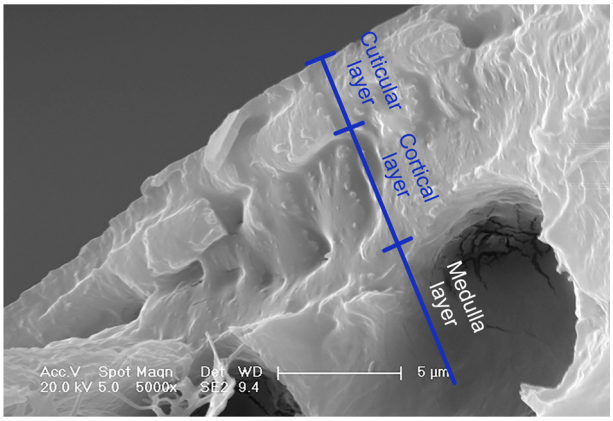

Fig. 2. Layered structure of reindeer foot fur.

According to the morphology and structure, can we distinguish the fur of reindeer on different parts of the foot? With regard to numeric features, Hicks pointed out that the difference of medulla ratios can play a role in fur identification. What is the effect of the different medulla index (MI) between reindeer fur and other animals? In the aspect of function, Chernova et al. found through research that the difference in structure and MI on medulla layer of fur was related to its thermal insulation properties. What are the functions of reindeer foot fur in cold ice and snow environments? Consequently, the microstructure and elementary composition for the foot fur of reindeer were analyzed in this paper to study the functional mechanism of reindeer fur on different parts in the ice and snow environment and long-distance migration.

2. Materials and methods

The fur of reindeer is mainly composed of dense fuzz and bristles. The color of fur on the reindeer back is gray brown or chestnut brown in summer. Moreover, the color of fur is slightly lighter in winter, showing gray brown or gray brown. In this paper, the bristles of different parts of the reindeer foot was selected. The reindeer, takes off fur twice a year, starts to molt in May and then begins to grow winter fur in September.

Before the test, the foot fur of reindeer was cleaned with distilled water and the filth and organic matters were removed from the surface of samples through the mixture of diethyl ether and ethyl alcohol (1:1). The micro observation on samples was conducted after natural drying.

The microstructure of foot fur was observed with the scanning electron microscope (SEM) equipped with an energy dispersive spectrometer (EDS) according to imaging technique and operating instruction. The images were compared to analyze the morphological structure of fur in fibular side, tibial side and planta pedis of the same foot and different positions of the same fur (Fig. 1). Then, the cross-sectional dimensions of fur of distal and medial parts were observed and measured. EDS energy spectrum analysis diagram and Fourier transform infrared spectroscopy (FTIR) were used to analyze the element content and composition of fur in fibular side, tibial side and planta pedis.

Table 1
Macro and micro morphology of fur on different foot parts (fibular side, tibial side and planta pedis) of reindeer.

Foot parts	Fibular side		Tibial side		Planta pedis	
Parameters	Distal part	Medial part	Distal part	Medial part	Distal part	Medial part
Color	Black	White	Gray	Gray	White	White
Diameter (μm)	146.05 ± 5.15	152.15 ± 5.36	134.58 ± 4.96	141.14 ± 3.44	102.11 ± 3.17	109.97 ± 3.81
MI (%)	70.35	77.88	81.79	88.08	76.18	—
Cross-sectional shape	Ellipse		Ellipse		Ellipse	

Note. Because of the existence of non-medullated segment in the medial part of fur of planta pedies, MI was not counted and expressed as "-".

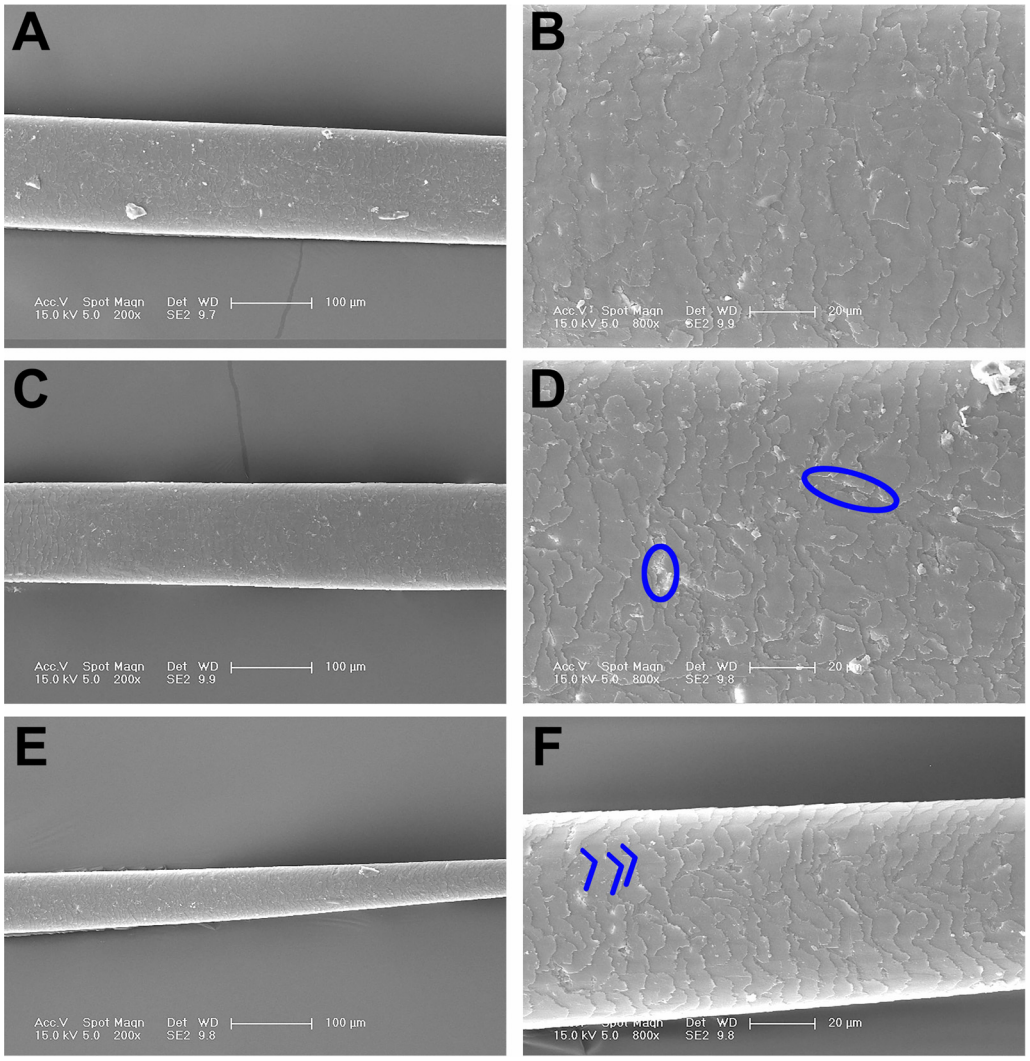

Fig. 3. Fur on the fibular side of foot A. Proximal part of fur (200×). B. Proximal part of fur (800×). C. Medial part of fur (200×). D. Medial part of fur (800×). E. Distal part of fur (200×). F. Distal part of fur (800×). The scales were worn in the circle, and the lines represented the scale wave.

2.1. Samples

Two healthy and adult male reindeer at the age of 8 came from the Ewenki nationality living in Genhe City of China. The samples, belonged to Rangifer tarandus phylarchus, did not receive any surgical treatment or other invasive operations. The fur from the right posterior foot of reindeer was cut off from the root with a surgical knife. Ten furs were collected from fibular side, tibial side and planta pedis of the foot on each sample respectively.

2.2. Scanning electron microscope (SEM)

Before the test, the filth was removed from the surface of fur. Then, the samples were plated in a vacuum chamber for gold plating (Edwards sputter coater S150 B) after the natural withering of fur. In order to observe the form of scales on cuticular layer, the 1000 B SEM (Philips XL30 ESEM-FEG, Germany) was used for inspection. The scanning electron microscope worked within the range of 5.0 KV. The micro observation was conducted on the surface of fur under the magnification times of 200× and 800×. Besides, the energy dispersive spectrometer (EDS) with a resolution ratio of 6 nm provided chemical composition of fur samples inside SEM.

In order to observe the cross-sectional structure of fur, the fur was cut off along the cross section with a surgical knife in liquid nitrogen. The scanning electron microscope was used to observe the cross section within the range of 800×-20000×.

2.3. Infrared spectra analysis

FTIR was used to analyze the composition of fur on different foot parts. Ten furs were collected from fibular side, tibial side and planta pedis of the foot on two samples. In order to remove the filth on the surface of fur, the samples were washed repeatedly with distilled water and placed on a clean white paper for natural withering. At the time of FTIR analysis, the foot fur of reindeer was smashed and ground into fine powder which was spread on the glass sheet evenly and compacted to form samples. The composition was tested through Shimadzu FNR-8400 S (Shimadzu Corporation, Kyoto, Japan) at room temperature, with the test frequency within the range of 400-4000 cm^{-1}.

2.4. Fur morphology

The measurement indexes are shown below:

- The proximal part of fur is located at the 1/4 position away from root, the medial part is located at the middle of fur shaft and the distal part is located at the 1/4 position away from tip.
- The maximum diameter of distal, medial and proximal parts of fur.

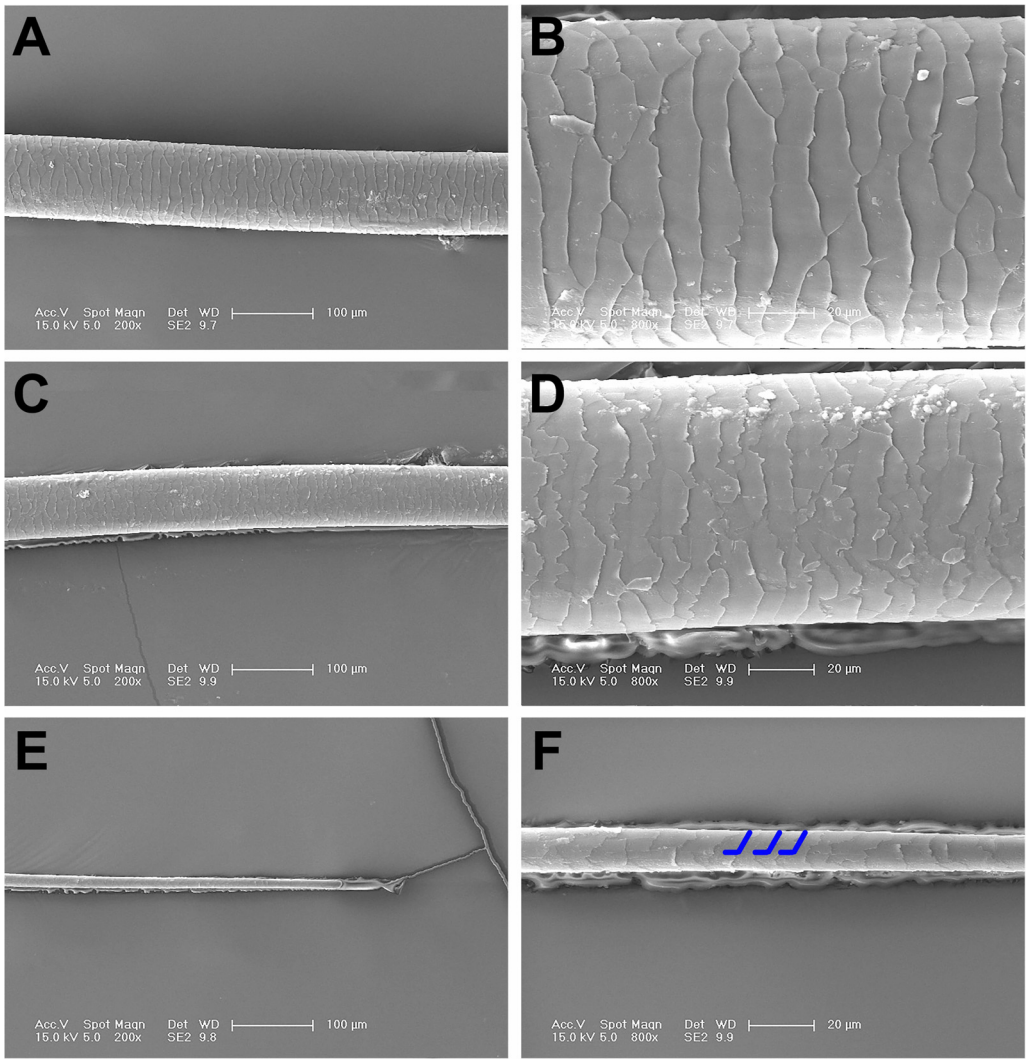

Fig. 4. Fur on the tibial side of foot A. Proximal part of fur (200×). B. Proximal part of fur (800×). C. Medial part of fur (200×). D. Medial part of fur (800×). E. Distal part of fur (200×). F. Distal part of fur (800×). The lines represented the scale wave.

- MI is the ratio between width and maximum diameter on the medulla layer of the same position.

3. Results and discussion

3.1. Macro and micro features of foot fur

The average length of fur of fibular side, tibial side and planta pedis were 17.13 mm, 24.52 mm and 43.86 mm, respectively. According to the calculation method of MI proposed by Sato et al., MI is the ratio between the diameter of medulla layer and that of fur at the position of maximum diameter (Sato et al., 2006). MI of human fur is less than 33.33%, that of hair for brown bears is about 36.00% and that of fur for dogs is about 60.00% (Sahajpal et al., 2008). The detailed dimensions of fur on different foot parts (fibular side, tibial side and planta pedis) of reindeer are shown in Table 1. The fur MI of polar animals is relatively large, which is related to its function of heat preservation (Chernova, 2002). MI was high for fur on tibial side and fibular side of reindeer, so the fur of tibial side and fibular side played an important role in heat preservation. It was found in researches that the dark fur at root and middle could absorb as much solar heat as possible, while the white fur at tip could reduce the heat loss on body surface (Koon, 1998). The fur on the fibular side of reindeer was black at root and middle and white at the tip (Fig. 1). This color distribution was conducive to the heat preservation of reindeer foot. The fur of tibial side and planta pedis was curved and rough, while that of fibular side was smooth.

3.2. Micro structure of foot fur

The fur is characterized by stratified structure. Many researches showed that the fur was mostly divided into 3 layers (Monica et al., 2015), namely cuticular layer, cortical layer and medulla layer. Similarly, the cross section for foot fur of reindeer was also divided into 3 layers in this paper, as shown in Fig. 2.

3.2.1. Surface morphology

The fur can avoid external mechanical trauma and protect the body. The cuticular layer, involved in the mechanical protection of fur, can form a “sac” that wraps cortical cells and fragile medulla layer (Nowak, 1998). The scales of cuticular layer include ovate, acuminate, elongate, dentate and flattened types, etc (Nason, 1948). Under the action of external environment, some types of fur scales may be worn. For example, the regular and flattened scale may turn into the scale in the type of irregular wave due to abrasion, even with the cuticular layer exfoliating completely (Srinivasan and Chakravarthy, 2016). The abrasion of scales can reflect the protective function of fur to a certain extent.

As shown in Fig. 3, the fur of fibular side covered the annular scales

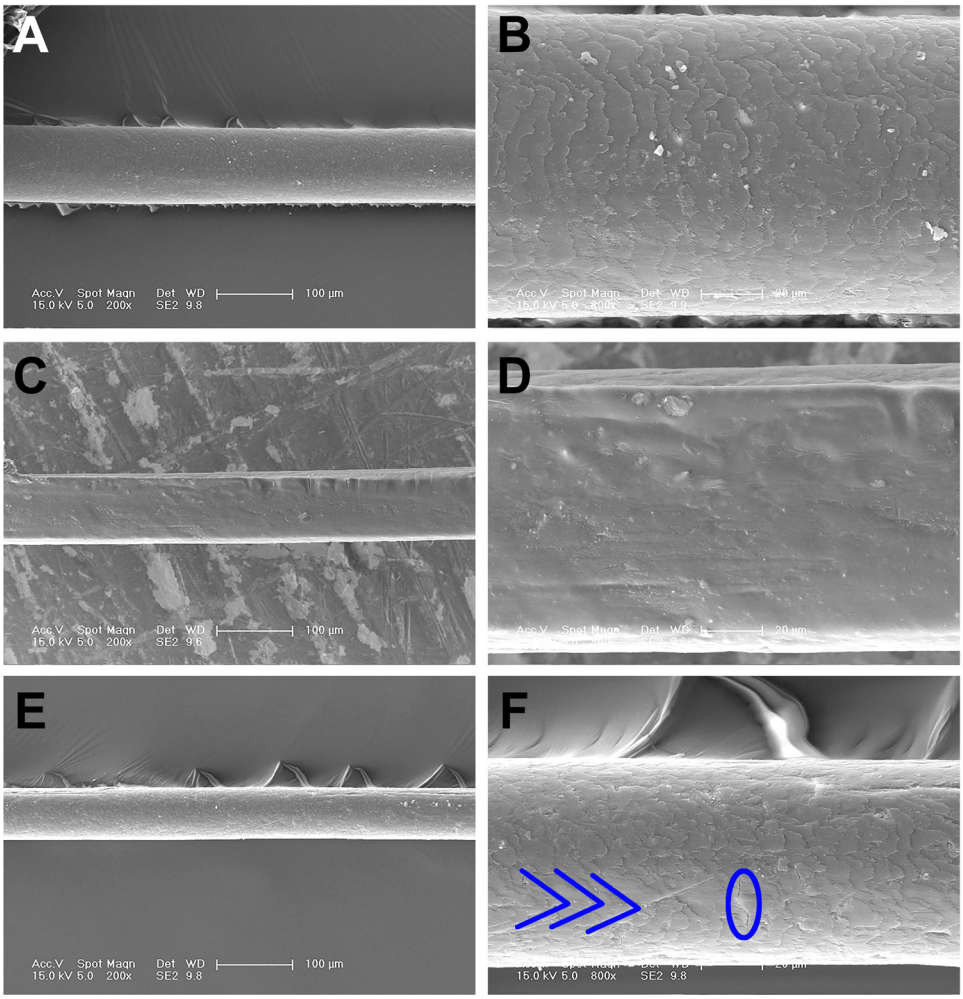

Fig. 5. Fur of planta pedis A. Proximal part of fur (200×). B. Proximal part of fur (800×). C. Medial part of fur (200×). D. Medial part of fur (800×). E. Distal part of fur (200×). F. Distal part of fur (800×). The scales were worn in the circle, and the lines represented the scale wave.

that were distributed axially and overlapped in order. All the scales were in the type of irregular wave, with cracked scales on the surface. This was mainly caused by mild wear, which reflected the positive role played by fur scales on fibular side in executing the protective function. As shown in Fig. 4, the scales of fur on tibial side included mosaic type at proximal part, irregular wave type at the medial part and coronary type at the distal part. The scales had smooth edge with little abrasion. As shown in Fig. 5, the scales at the proximal part and distal part of fur on planta pedis showed the type of irregular wave. The cuticular layer at the medial part of fur exfoliated and thus the cortical layer was exposed. There were cracked scales and slip lines at the distal part, with a few of scales damaged. This reflected that the fur of planta pedis played an important role in protecting planta pedis and the effect at the medial part of fur was most obvious.

The scales are distributed on different modes to play different roles. The fur of planta pedis is worn most seriously, which indicates that the fur of planta pedis plays a role in protecting planta pedis. In winter, the foot of reindeer is the only part in contact with the icy and snowy ground (Zhang et al., 2017). The scales at the distal part of fur on planta pedis are distributed more closely compared with those of other parts. And the scale wave fluctuates more greatly. This special structure may have the skidproof function during the movement of reindeer. It was found in researches that the foot fur of reindeer had a direct contact with external environment at the medial part and distal part through some special structures (Timisjärvi et al., 1984; Zhang et al., 2017). Therefore, we also observed the cross sections at the distal part and medial part of foot fur.

3.2.2. *Cross-sectional structure*

All the cross sections of foot fur were elliptical structures, but the ratios of minimum diameter and maximum diameter were different. As shown in Fig. 6, the ratios of minimum diameter L_1 and maximum diameter L_2 at the distal part of fur on fibular side, tibial side and planta pedis were 39.11%, 50.10% and 56.30% respectively. The ratios of minimum diameter L_1 and maximum diameter L_2 at the medial part of fur on fibular side, tibial side and planta pedis were 56.21%, 52.54% and 62.46% respectively. The ratio of minimum diameter and maximum diameter for the cross section at the medial part of foot fur was larger than that at the distal part.

The cortical layer is composed of thin and straight cortical cells that are distributed closely. There are abundant fiber structures inside cortical cells (Kelch et al., 2000). The tensile strength and elasticity of fur depend on the development level of cortical layer. Located at the medial part of fur on planta pedis, the non-medullated segment is fully composed of cortical layer, because this part contacts with the external environment most frequently and is worn most seriously. The existence of non-medullated segment strengthens the capability of hair on planta pedis so as to resist to external abrasion and protect fur and planta pedis.

The medulla layer of fibular side and tibial side belongs to porous foaming structure, which separates the medulla layer as an independent hollow “interlayer”. For example, the hollow fur of polar bears has the

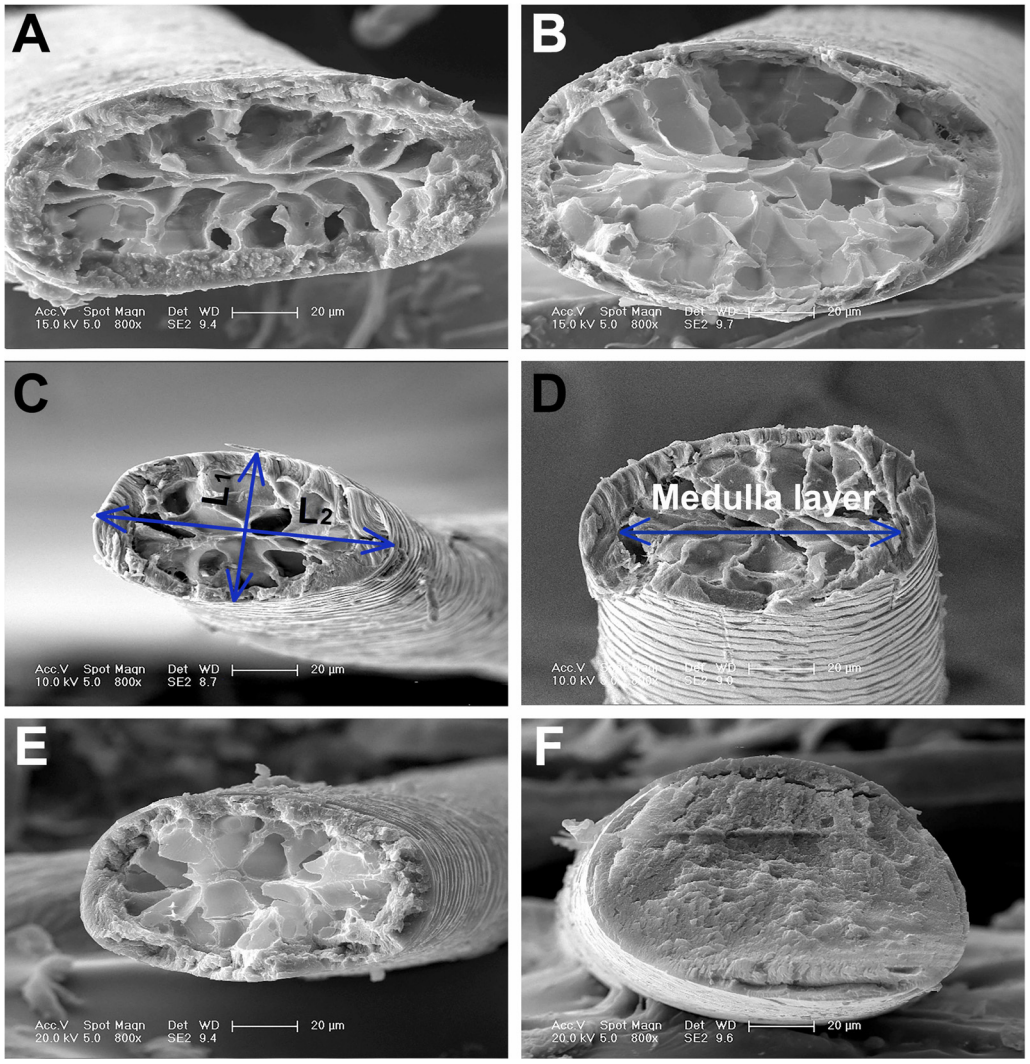

Fig. 6. Cross sections of fur on different foot parts A. Distal part of fur on fibular side. B. Medial part of fur on fibular side. C. Distal part of fur on tibial side. D. Medial part of fur on tibial side. E. Distal part of fur on planta pedis. F. Medial part of fur on planta pedis.

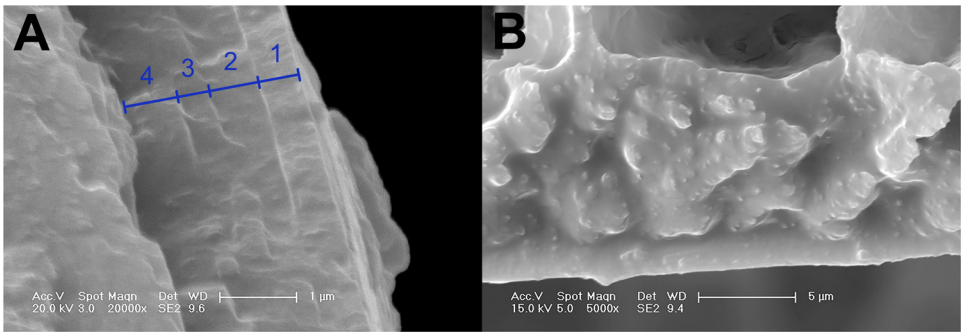

Fig. 7. Layered structure of cuticular layer and structure of cortical layer.

effect of “daylight transducer” and plays the role of heat preservation (Engelhardt and Sarsour, 2015; Tributsch et al., 1990). Hence, we thought that the hollow “interlayer” in the foot fur of reindeer played the role of heat preservation in clod winter. Reindeer are good at swimming (Korytin, 2001). Such a porous foam structure of foot fur could also increase reindeer’s buoyancy and facilitate swimming.

3.2.3. Layered structure

Fig. 7 showed the layered structure of cuticular layer and the structure of cortical layer in the foot fur of reindeer. It was observed from SEM results that the cortical layer was a multilayered structure which was divided into 4 layers combining with each other closely, as shown in Fig. 7a. A physical structure without obvious layered structure (Fig. 7b).

3.3. Material composition

The function of fur is not only related to structure, but also related

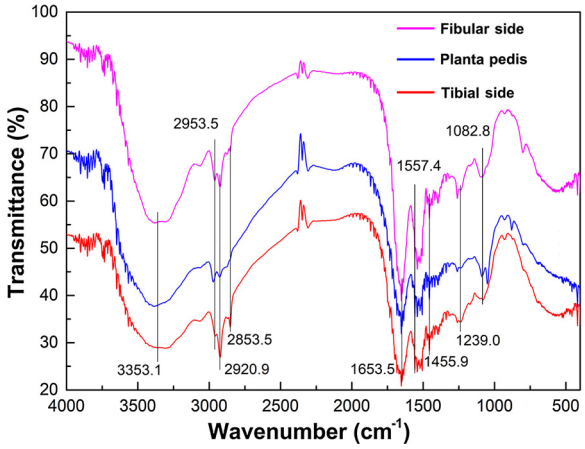

Fig. 8. Infrared absorption spectrum of foot fur.

Table 2
Contents of elements on different parts of foot fur (%).

Element	C	N	O	S
Fur of fibular side	65.77	10.50	21.04	2.68
Fur of tibial side	67.93	9.31	19.66	3.11
Fur of planta pedis	67.45	8.59	20.15	3.81

to chemical composition (Sundaramoorthi et al., 2017). The element and material composition of the foot fur were analyzed through EDS analysis and FTIR analysis. The Fourier transform infrared spectroscopy can be used for the qualitative analysis on the compound that absorbs infrared light. As shown in Fig. 8, the infrared spectral images of foot fur in 3 parts were similar and the positions and shapes of all absorption peaks and the positions of characteristic peaks were basically the same.

The results of FTIR image for foot fur showed that the absorption peaks appeared at the positions of 3353.1, 2949.5, 2853, 2307.3, 1653.5, 1557.4, 1455.9 and 1239 cm^{-1}. The absorption peak at the position of 3353.1 cm^{-1} was N—H contraction band (Amide A band). The absorption peaks at the positions of 2949.5 and 2853 cm^{-1} were caused by C—H stretching vibration of methyl (CH_3) and methylene (CH_2) respectively (Akhtar et al., 1997; Huang et al., 2018a, 2018b, 2018c, 2018d). The strong absorption band at the position of 1635.5 cm^{-1} was mainly the C═O stretching vibration band (Amide I band) of peptide chain (CN—NH) in protein molecule of keratinocytes (Lyman and Murraywijelath, 2005). The absorption band at the position of 1557.4 cm^{-1} was primarily the N—H bending vibration band (Amide II band) of protein (Chen et al., 2006; Likun et al., 2018; Walsh et al., 2007;). The absorption band at the position of 1455.9 cm^{-1} was caused by CH_3 bending vibration of amino acid (Bantignies et al., 2010). The absorption band at the position of 1239 cm^{-1} was caused by C—N stretching vibration (Amide III band). The position of 1082.8 cm^{-1} was the absorption band caused by S—O stretching vibration of cystine oxide (Walsh et al., 2007).

The energy spectrum analysis is of great significance in the research of material composition. In this paper, the infrared spectra technology was only used for the qualitative analysis on the composition of organic matters in fur. Therefore, it was necessary to measure C, N, O and S elements of the foot fur of reindeer through energy spectrum analysis, with the contents of fur elements on different parts shown in Table 2.

It was observed from the results of chemical composition analysis that the chemical compositions of foot fur were different on different parts. Thereinto, C was the main element (fur of fibular side: C-65.77%, fur of tibial side: C-67.93% and fur of planta pedis: C-67.45%). The content of sulfur for the fur of planta pedis was 3.81%, higher than that of other parts (fur of fibular side: S-2.68% and fur of tibial side: S-3.11%).

4. Conclusions

The structure, morphology, material composition and functional analysis of furs on different parts of reindeer foot were studied through scanning electron microscope, infrared spectroscopy and energy spectrum analysis. The foot fur favour the remarkable long-distance migrating and swimming abilities of reindeer, which could play the roles of protect, heat preservation and increase buoyancy.

The foot fur of reindeer was divided into 3 layers, namely cuticular layer, which was composed of multilayered structure, cortical layer, which was a physical structure, and medulla layer. There was a non-medullated segment at the medial part of fur on planta pedis. This was a structure that can enhance the tensile strength and elasticity of fur to protect fur and plata pedis. The medulla layer of fibular and tibial sides mostly showed a porous foam structure. Meanwhile, MI of fur of fibular side and tibial side at distal part was 70.35% and 81.79%, respectively, and that at medial part was 77.88% and 88.08%. The large MI and the porous structure of fur played the function of heat preservation in cold winter. Meanwhile, the porous foam structure of foot fur could also increase reindeer's buoyancy and facilitate swimming.

There was a difference in the surface structure of fur on different parts of the same foot and different positions of the same fur. The scales of fur on tibial side had smooth edge, with the scale structure in mosaic and coronary types, etc. The fur of fibular side and planta pedis was in the type of irregular wave due to abrasion to different degrees. Thereinto, the fur of planta pedis was worn most seriously. The scale layer at the medial part of fur exfoliated and thus the cortical layer was exposed, indicating that the hai of plata pedis played an important role in protecting planta pedis.

The ratios of minimum diameter and maximum diameter at the medial part of fur on fibular side, tibial side and planta pedis were 56.21%, 52.54% and 62.46% respectively, higher than those at the distal part.

The infrared spectral images of foot fur in fibular side, tibial side and planta pedis were similar and the positions and shapes of all absorption peaks and the positions of characteristic peaks were basically the same. The element content of foot fur varied on different parts. The content of sulfur for the fur of planta pedis was higher than that of other parts.

Funding

This work was supported by the National Natural Science Foundation of China [grant numbers 51675221]; the Science and Technology Development Planning Project of Jilin Province of China [grant numbers 20180101077JC] and the Science and Technology Research Project in the 13th Five-Year Period of Education Department of Jilin Province [grant numbers JJKH20190134KJ].

CRediT authorship contribution statement

Rui Zhang: Conceptualization. **Guoyu Li:** Writing - original draft. **Ruiduo Pan:** Data curation. **Qiang Wang:** Data curation, Software. **Jianqiao Li:** Resources.

Declaration of Competing Interest

All authors declare no conflict of interest.

References

Alam, F., Ahmad, M., Zafar, M., Shinwari, M.I., Luqman, M., Novruz, N.E., Sultana, S., Ullah, F., Ahmad, M., 2019. Intraspecific variation in spermoderm pattern of tribe Acacieae (Mimosoideae) using scanning electron microscopy techniques. Microsc. Res. Technol. 82 (4), 114–121.

Ahmed, Y.A., Ali, S., Ghallab, A., 2018. Hair histology as a tool for forensic identification of some domestic animal species. EXCLI J. 17, 663–670.

Akhtar, W., Edwards, H.G., Farwell, D.W., Nutbrown, M., 1997. Fourier-transform Raman spectroscopic study of human hair. Spectrochim. Acta A 53 (7), 1021–1031.
Anderson, M.J., 2001. The use of hair morphology in the classification of galagos (Primates, subfamily galagoninae). Primates 42 (2), 113–121.
Anzures, F., Gaytán, L., Macías-Cruz, U., Avendaño-Reyes, L., García, J.E., Mellado, M., 2019. Milk yield and hair coat characteristics of Holstein cows in a hot environment. Trop. Anim. Health Prod. 51 (5), 1253–1257.
Aris, F.P., George, C., 2008. Morphology of the hair in the goat breed capra prisca. J. Anim. Vet. Adv. 7 (9), 1142–1145.
Banfieldal, A.W.F., 1957. The plight of the barren ground Caribou. Oryx 4 (1), 5–20.
Bantignies, J.L., Fuchs, G., Carr, G.L., Williams, G.P., Lutz, D., Marull, S., 2010. Organic reagent interaction with hair spatially characterized by infrared microspectroscopy using synchrotron radiation. Int. J. Cosmetic Sci. 20 (6), 381–394.
Cain, J.W., Krausman, P.R., Rosenstock, S.S., Turner, J.C., 2006. Mechanisms of thermoregulation and water balance in desert ungulates. Wildl. Soc. Bull. 34 (3), 570–581.
Chen, Y.J., Cheng, Y.D., Liu, H.Y., Lin, P.Y., Wang, C.S., 2006. Observation of biochemical imaging changes in human pancreatic cancer tissue using Fourier-transform infrared microspectroscopy. Biomed. J. 29 (5), 518–527.
Chernova, O.F., 2002. Architectonic and diagnostic significance of hair cuticle. Biol. Bull. Russ. Acad. Sci. 29 (3), 238–247.
Currey, J.D., 1999. The design of mineralised hard tissues for their mechanical functions. J. Exp. Biol. 202 (23), 3285–3294.
Engelhardt, S., Sarsour, J., 2015. Solar heat harvesting and transparent insulation in textile architecture inspired by polar bear fur. Energy Build. 103, 96–106.
Erdoğan, S., Villar, A.S., Pérez, W., 2016. Morphofunctional structure of the lingual papillae in three species of South American Camelids: alpaca, guanaco, and llama. Microsc. Res. Technol. 79 (2), 61–71.
Gilg, O., Kovacs, K.M., Aars, J., Fort, J., Gauthier, G., Grémillet, D., Ims, R.A., Meltofte, H., Moreau, J., Post, E., Schmidt, N.M., Yannic, G., Bollache, L., 2012. Climate change and the ecology and evolution of arctic vertebrates. Ann. N.Y. Acad. Sci. 1249 (1), 166–190.
Hausman, L.A., 1920. Structural characteristics of the hair of mammals. Am. Nat. 54 (635), 496–523.
Huang, L.K., Huang, Z.H., Li, Q., Zhang, T.X., Sang, N., 2018a. Framelet regularization for uneven intensity correction of color images with illumination and reflectance estimation. Neurocomputing 314, 154–168.
Huang, Z.H., Zhang, Y.Z., Zhang, T.X., Li, Q., Sang, N., 2018b. Spatially adaptive denoising for X-ray cardiovascular angiogram images. Biomed. Signal Process. Control 40, 131–139.
Huang, Z.H., Zhang, Y.Z., Li, Q., Zhang, T.X., Sang, N., Hong, H.Y., 2018c. Progressive dual-domain filter for enhancing and denoising optical remote-sensing images. IEEE Geosci. Remote Sens. Lett. 15 (5), 759–763.
Huang, Z.H., Li, Q., Zhang, T.X., Sang, N., Hong, H.Y., 2018d. Iterative weighted sparse representation for X-ray cardiovascular angiogram image denoising over learned dictionary. IET Image Process. 12 (2), 254–261.
Jacobsen, N.K., 1980. Differences of thermal properties of white-tailed deer pelage between seasons and body regions. J. Therm. Biol. 5 (3), 151–158.
Kelch, A., Wessel, S., Will, T., Hintze, U., Wepf, R., Wiesendanger, R., 2000. Penetration pathways of fluorescent dyes in human hair fibres investigated by scanning near-field optical microscopy. J. Microsc. 200 (3), 179–186.
Koon, D.W., 1998. Is polar bear hair fiber optic? Appl. Optics 37 (15), 3198–3200.
Korytin, N.S., 2001. On the distribution of reindeer in the middle and northern urals. Russ. J. Ecol. 32 (1), 58–60.
Likun, H., Zhenghua, H., Qian, L., Tianxu, Z., Nong, S., 2018. Framelet regularization for uneven intensity correction of color images with illumination and reflectance estimation. Neurocomputing 314, 154–168.
Lyman, D.J., Murraywijelath, J., 2005. Fourier transform infrared attenuated total reflection analysis of human hair: comparison of hair from breast cancer patients with hair from healthy subjects. Appl. Spectrosc. 59 (1), 26–32.
Meyer, W., Schnapper, A., Hülmann, G., 2006. The hair cuticle of mammals and its relationship to functions of the hair coat. J. Zool. 256 (4), 489–494.
Monica, B., Peric, T., Ajuda, I., Vieira, A., Grosso, L., Sara, B., Stilwell, G., Prandi, A., Comin, A., Tubaro, F., Mattiello, S., 2015. Hair coat condition: a valid and reliable indicator for on-farm welfare assessment in adult dairy goats. Small Rumin. Res. 123 (2-3), 197–203.
Nakayama, M., Tagashira, H., Konishi, S., Ogura, Kotaro., 2004. A direct electrochemical route to construct a polymer/manganese oxide layered structure. Inorg. Chem. 43 (26), 8215–8217.
Nason, E.S., 1948. Morphology of hair of eastern north American bats. Am. Midl. Nat. 39 (2), 345–361.
Noback, C.R., 2010. Morphology and phylogeny of hair. Ann. N. Y. Acad. Sci. 53 (3), 476–492.
Nowak, B., 1998. Contents and relationship of elements in human hair for a non-industrialised population in Poland. Sci. Total Environ. 209 (1), 0–68.
Oli, M.K., 1993. A key for the identification of the hair of mammals of a snow leopard (Panthera uncia) habitat in Nepal. J. Zool. 231 (1), 71–93.
Payne, R.C., Hutchinson, J.R., Robilliard, J.J., Smith, N.C., Wilson, A.M., 2005. Functional specialisation of pelvic limb anatomy in horses (Equus callabus). J. Anat. 206 (6), 557–574.
Ricca, M.A., Weckerly, F.W., Duarte, A., Williams, J.C., 2012. Range expansion of non-indigenous caribou in the Aleutian archipelago of Alaska. Biol. Invasions 14 (9), 1779–1784.
Rymer, T.L., Kinahan, A.A., Pillay, N., 2007. Fur characteristics of the African ice rat otomys sloggetti robertsi: modifications for an alpine existence. J. Therm. Biol. 32 (7), 428–432.
Sahajpal, V., Goyal, S.P., Jayapal, R., Yoganand, K., Thakar, M.K., 2008. Hair characteristics of four Indian bear species. Sci. Justice 48 (1), 8–15.
Sato, H., Matsuda, H., Kubota, S., Kawano, K., 2006. Statistical comparison of dog and cat guard hairs using numerical morphology. Forensic Sci.Int. 158 (2), 94–103.
Scholander, P.F., Walters, V., Irving, H.L., 1950. Body insulation of some arctic and tropical mammals and birds. Biol. Bull. 99 (2), 225–236.
Srinivasan, G., Chakravarthy, R.S., 2016. Scanning electron microscopy of hair treated in hard water. Int. J. Dermatol. 55 (6), 344–346.
Sundaramoorthi, K., Sethu, G., Ethirajulu, S., Raja, M.P., 2017. Efficacy of metformin in human single hair fibre by ATR-FTIR spectroscopy coupled with statistical analysis. J. Pharm. Biomed. Anal. 136, 10–13.
Taru, P., Backwell, L., 2013. Identification of fossil hairs in Parahyaena brunnea coprolites from middle pleistocene deposits at gladysvale cave, South Africa. J. Archaeol. Sci. 40 (10), 3674–3685.
Timisjärvi, J., Nieminen, M., Sippola, A.L., 1984. The structure and insulation properties of the reindeer fur. Comp. Biochem. Physiol. A Comp. Physiol. 79 (4), 601–609.
Tributsch, H., Goslowsky, H., Küppers, U., Wetzel, H., 1990. Light collection and solar sensing through the polar bear pelt. Sol. Energy Mater. 21 (2-3), 219–236.
Wallis, R.L., 1993. A key for the identification of guard hairs of some Ontario mammals. Can. J. Zool. 71 (3), 587–591.
Walsh, M.J., German, M.J., Singh, M., Hubert, M., Hammiche, A., Kyrgiou, M., Stringfellow, H.F., Paraskevaidis, E., Martin-Hirsch, P.L., Martin, F.L., 2007. IR microspectroscopy: potential applications in cervical cancer screening. Cancer Lett. 246, 0–11.
Wareing, K., Tickle, P.G., Stokkan, K.A., Codd, J.R., Sellers, W.I., 2011. The musculoskeletal anatomy of the reindeer (Rangifer tarandus): fore- and hindlimb. Polar Biol. 34 (10), 1571–1578.
Zhang, R., Qiao, Y., Ji, Q.L., Ma, S.S., Li, J.Q., 2017. Macro-microscopic research in reindeer (Rangifer tarandus) hoof suitable for efficient locomotion on complex grounds. J. Vet. Res. 61 (2), 223–229.